14 Making Invasion Models Useful for Decision Makers: Incorporating Uncertainty, Knowledge Gaps and Decision-making Preferences

Denys Yemshanov,[1] Frank H. Koch[2] and Mark Ducey[3]

[1]*Natural Resources Canada, Canadian Forest Service, Great Lakes Forestry Centre, Sault Ste. Marie, Ontario, Canada;* [2]*USDA Forest Service, Southern Research Station, Eastern Forest Environmental Threat Assessment Center, Research Triangle Park, North Carolina, USA;* [3]*Department of Natural Resources and the Environment, University of New Hampshire, Durham, New Hampshire, USA*

Abstract

Uncertainty is inherent in model-based forecasts of ecological invasions. In this chapter, we explore how the perceptions of that uncertainty can be incorporated into the pest risk assessment process. Uncertainty changes a decision maker's perceptions of risk; therefore, the direct incorporation of uncertainty may provide a more appropriate depiction of risk. Our methodology borrows basic concepts from portfolio valuation theory that were originally developed for the allocation of financial investments under uncertainty. In our case, we treat the model-based estimates of a pest invasion at individual geographical locations as analogous to a set of individual investment asset types that constitute a 'portfolio'. We then estimate the highest levels of pest invasion risk by finding the subset of geographical locations with the 'worst' combinations of a high likelihood of invasion and/or high uncertainty in the likelihood estimate. We illustrate the technique using a case study that applies a spatial pest transmission model to assess the likelihood that Canadian municipalities will receive invasive forest insects with commercial freight transported via trucks. The approach provides a viable strategy for dealing with the typical lack of knowledge about the behaviour of new invasive species and generally high uncertainty in model-based forecasts of ecological invasions. The technique is especially useful for undertaking comparative risk assessments such as identification of geographical hot spots of pest invasion risk in large landscapes, or assessments for multiple species and alternative pest management options.

* Corresponding author. E-mail: Denys.Yemshanov@NRCan-RNCan.gc.ca

Uncertainty in Biological Invasions

Probabilistic spatial models have been used to assess the potential for, and impacts from, ecological invasions (Rafoss, 2003; Koch *et al*., 2009; Pitt *et al*., 2009; Yemshanov *et al*., 2009a,b; Prasad *et al*., 2010; Venette *et al*. 2010; Koch and Yemshanov, Chapter 13 in this volume). Such models offer the capacity to depict fine-scale variations in key environmental and biological parameters that may influence the dynamics of invasive alien species in a landscape. However, parameters in these models require certain statistical assumptions, so when these models are extrapolated in geographical space, uncertainty that is associated with underlying model structure, parameters and data is propagated into pest risk forecasts and maps.

Description of the invasion process in probabilistic terms provides a technical means to represent uncertainties in the events that lead to invasion. Probabilistic invasion models commonly include randomization algorithms to represent the uncertain course of an invasion. For example, forecasts of where an invasive alien organism might be introduced and subsequently spread may include random elements. Alternatively, randomization algorithms can be used to draw plausible values repeatedly from statistical distributions of model inputs to measure the resultant variation in model outputs. This approach is known more generally as Monte Carlo analysis. Numerous randomized simulations of the invasion process provide a set of possible invasion outcomes (Koch *et al*., 2009; Pitt *et al*., 2009; Yemshanov *et al*., 2009a). The model outputs (e.g. an invasive alien species' presence/absence or density at a site by a specified time) can be analysed statistically to determine an expected outcome or the extent of variation among outcomes. These statistics can, for example, provide important insights about managing an invasion in the face of uncertainty or targeting research to alleviate some of the uncertainty.

In this chapter, we focus on relatively simple techniques that help incorporate the uncertainty that is typically generated by probabilistic spatial models into the output risk estimates (i.e. risk maps) for invasive alien pests. Note that the 'risk' we are modelling in this example is the likelihood of the arrival of wood- and bark-boring insects without considering the level of impact. Conceptually, our approach would apply to other aspects of ecological invasions. Because our approach is from a decision maker's perspective, the final estimates should also reflect how the uncertainty in the invasion forecasts might change a decision maker's expectations of invasion outcomes.

Perceptions of Uncertainty in Model-based Pest Risk Assessments

Uncertainty is an inevitable component of invasion forecasts but can be challenging for pest risk managers (i.e. biosecurity professionals and others tasked with managing pest incursions) to factor into their decision-making processes. One of the biggest impediments has been the lack of techniques to directly incorporate uncertainty into the prioritization of risks for decision makers. Notably, human perceptions of 'more certain' versus 'less certain' outcomes are different in a decision-making context (Kahneman and Tversky, 1979; Kahneman *et al*., 1982); a decision maker's perception of uncertainty embedded in a forecast of pest risk could change his or her priorities for action. Perceptions of uncertainty differ among people. For example, given a choice between two alternative scenarios with the same estimated probabilities of pest arrival, a cautious risk manager would assign higher priority for action to the scenario with more certainly estimated values. This type of behaviour is commonly called 'risk-averse' in economic literature: risk-averse individuals always prefer the more certain option from alternative choices with the same expected outcome (Arrow, 1971; Gigerenzer, 2002; Shefrin and Belotti, 2007). For example, the risk-averse investor would prefer a stock with a 3 ± 0.5% annual return on investment over the stock with a 3 ± 4% annual return. Conversely, 'risk-tolerant' or 'risk-seeking'

investors would prefer the more variable stock because this stock has a greater potential to outperform its historical average return in the short term than the more consistent stock.

The meaning of 'risk' in investments is different from how it is typically understood in pest risk modelling (i.e. as shorthand for the likelihood of arrival, establishment and spread, and the magnitude of impacts). Indeed, risk aversion might be better characterized as aversion to uncertainty in the elements of the invasion being modelled. This terminology is admittedly ambiguous, but 'risk aversion' also implies that a pest risk manager would generally assign lower priority for action to estimates of pest invasion risk that are comparatively more uncertain. However, for information-gathering purposes, decision makers may reverse their priorities and become more risk-tolerant. For example, a pest risk model to plan a pest survey in a heterogeneous landscape may show two locations where the presence of an invasive alien species is equally probable but the estimate for one location is more uncertain than for the other. For the risk-tolerant manager, locations with more uncertain risk estimates would be assigned a higher priority for survey (Yemshanov *et al.*, 2010) because these locations would provide more knowledge-gaining opportunities. Results from surveys in these locations also could help to reduce some of the uncertainty associated with the model parameters or inputs.

Ideally, the risk assessor would use an algorithm to consistently adjust outputs from a probabilistic invasion model to support decision making. The adjustment would depend on the amount of uncertainty in the outputs and a basic understanding of the decision maker's perceptions of uncertainty. Potential adjustments can be visualized by plotting the model-based estimates of risk in two dimensions: the mean likelihood of invasion (i.e. across all model replications) against the uncertainty of that likelihood estimate. For example, a pest's estimated mean arrival rate for each location of interest is plotted against the variance in Fig. 14.1a.

When uncertainty is ignored and the action priorities (e.g. selection of sites for surveillance) are based solely on the mean invasion likelihood values, the dividing boundaries between high- and low-priority locations can be depicted in the mean–variance space as lines with constant mean likelihood values parallel to the *x*-axis (Fig. 14.1b). In this case, the amount of variance in the likelihoods of pest invasion does not affect the decision-making choice. If decision makers assign higher priorities to more certain estimates of pest invasion likelihood (i.e. are 'risk-averse'), the lines that delineate action priority levels will be curved relative to the *x*-axis (Fig. 14.1c), so the locations with more certainly defined estimates of invasion likelihood would receive higher relative priority and vice versa. Alternatively, when a decision maker's objective is to gain more information about an invader's behaviour, or when uncertainty in the invasion likelihood values is believed to increase the overall level of decision-making priority (i.e. the decision maker is 'risk-seeking'), the locations with higher variance will be assigned a higher priority. In this case, the lines delimiting the priority levels would be curved relative to the *x*-axis in an opposite direction (Fig. 14.1d).

Portfolio Valuation Techniques and Pest Risk Assessment

The concepts depicted in Fig. 14.1 are strikingly similar to the financial asset valuation process which has been studied in detail and has produced a corresponding analytical framework (Arrow, 1971; Elton and Gruber, 1995). To illustrate how this framework may be translated to invasive species modelling, consider a hypothetical example of a geographical assessment of pest invasion likelihood, where a spatial invasion model has forecast the potential spread of a newly documented pest. Knowledge about the invader's behaviour in its new environment remains limited, so the

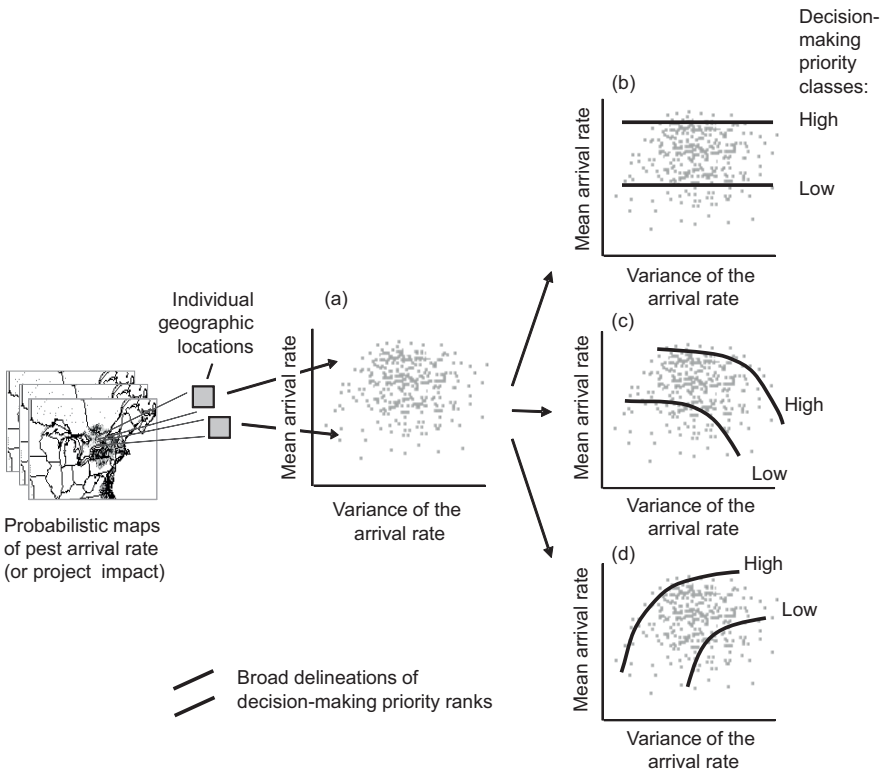

Fig. 14.1. Delineation of decision-making priorities with respect to mean pest arrival rate and uncertainty: (a) depicting individual geographical locations (i.e. map cells) as points in the dimensions of mean pest arrival rate and variance; (b) decision making is based solely on the mean values regardless of the amount of variance in the arrival rate estimates (points above the 'high' line are a high priority, those below the 'low' line a low priority and points between the lines are a medium priority); (c) decision making assigns higher priority to estimates with higher variance; (d) decision making is risk-averse, so more certain estimates of the pest arrival rate receive higher priority.

spatial model represents key parameters that characterize the species' expected behaviour in distributional form. Multiple randomized simulations generate, for each location (i.e. individual map cells, in this example), a multitude of estimated pest arrival rates within a specified time. For each location, the invader's estimated mean arrival rate and the uncertainty of that estimate (i.e. the variance of the simulated mean) can be calculated. Results for multiple locations can be plotted on a mean–variance graph (Fig. 14.1). Plots generally show the points as an amorphous cluster termed a 'cloud' (Fig. 14.1a).

Locations for resource deployment (e.g. to monitor the ongoing spread of the invader) are prioritized by finding the locations that have the 'most extreme' combinations of mean arrival rates and associated uncertainties. What constitutes 'most extreme' depends on the decision maker's perception of uncertainty. For example, uncertainty might increase (Fig. 14.1c) or decrease (Fig. 14.1d) the priority for action at a location. Regardless, the combinations of mean arrival rate and uncertainty characterize locations within the mean–variance cloud. For instance, a relatively low arrival rate that is highly

uncertain would place a location on the outer (i.e. most extreme) boundary of the point cloud. Notably, this combination is analogous to finding the 'non-dominant' portfolio set in financial asset allocation when considering mean net financial returns and their volatilities (i.e. the variances of the net return values). In our case, the likelihood that the threatening pest will arrive at a previously pest-free location is analogous to the concept of 'net return', while the uncertainty of that likelihood estimate is analogous to 'volatility' (Arrow, 1971; Elton and Gruber, 1995).

In pest risk modelling, a set of individual geographical locations (e.g. map cells or polygons) within a region is analogous to a set of individual 'portfolios', where each 'portfolio' is characterized by an associated distribution of estimated net returns (i.e. analogous to model-based likelihoods of pest arrival). Commonly, we rank these locations so the highest rank would denote the most extreme combination of arrival rate and uncertainty. As we perceive the process, decision makers will continue to select the most highly ranked sites until a budget limit is reached. Lines that distinguish high-priority locations (i.e. those that need immediate management action) from lower-priority locations (i.e. where action could be deferred) can be drawn through the mean–variance cloud. These limits are represented as convex lines (i.e. 'frontiers') at user-defined boundaries within the mean–variance clouds. Figure 14.1c illustrates the general shape of these lines when the decision maker is risk-averse and Fig. 14.1d illustrates the general shape when the decision maker is risk-tolerant.

In portfolio allocation, the usual objective is to select a few portfolio combinations from a theoretically infinite set that have the desired trade-offs between net returns and their volatilities (Elton and Gruber, 1995). In our invasion risk modelling scenario, each portfolio represents a single geographical location, so their total number is finite. Under classical portfolio theory, allocation usually aims to define a single best-performing set of portfolios in financial terms (Ingersoll, 1987; Elton and Gruber, 1995). A single set is sufficient because it is assumed that any investment amount can be allocated simply in specified proportions to the set of portfolios. In geographical assessments of pest invasions, finding a single best-performing portfolio set would be analogous to identifying a small portion of the geographical region that combined the highest likelihoods of invasion and the highest variances of these estimates (or lowest, depending on decision-making goals).

In order to evaluate the rest of the map locations, we must subsequently define a hierarchy of best- to worst-performing portfolio sets for all map locations in a study area. To do this, the distribution of arrival rates for each of the n locations (i.e. square cells) in the map is evaluated to find a subset, $\aleph_1$, of locations with the most extreme combinations of arrival rate and associated uncertainty. In financial terminology, this subset is often called the 'non-dominant' or 'efficient' set. Once the non-dominant set $\aleph_1$ is found, it is assigned the highest priority rank of 1 and removed from set n temporarily. Next, a second non-dominant subset, $\aleph_2$, is determined from the rest of the map locations, $n - \aleph_1$, assigned a rank of 2, and so forth. The process is repeated until all sets of locations in the area of interest have been evaluated and assigned a priority rank. Conceptually, this technique follows an algorithm for finding nested non-dominant sets (Goldberg, 1989) and multi-attribute frontiers (Yemshanov *et al.*, 2013).

Finding Non-dominant Frontiers

Finding nested non-dominant sets, or efficient frontiers, represents the most critical step in the analysis because the set limits must simultaneously account for a decision maker's perceptions of uncertainty and the amount of variation in the data, and yet be computationally tractable. In this chapter, we demonstrate two relatively simple approaches based on the mean–variance frontier concept and the stochastic

dominance rule. We continue to draw upon the example that we established earlier. To briefly recap, an area of interest is divided into *n* grid cells (i.e. locations). A Monte Carlo simulation generates multiple estimates of the arrival rate of an invasive alien species into each cell. For each cell, we have an estimate of the mean arrival rate (i.e. the mean of all simulated values for that cell) and uncertainty in the arrival rate (i.e. the variance or standard deviation about the mean and the frequency distribution of arrival rates). Our goal is to help the decision maker select particular locations for action (e.g. conduct a survey for the invasive alien species).

Mean–variance frontier concept

The mean–variance frontier (MVF) concept is a visually appealing and simple technique. The mean arrival rate, $\bar{\psi}_j$, for a location *j* is plotted against the standard deviation of the arrival rate, $\sigma(\psi_j)$, which serves as a measure of uncertainty (Fig. 14.2a). All geographical locations are plotted on the same graph. Instead of using variance as the measure of uncertainty, we use the standard deviation because it increases monotonically with the variance, spreads points along the uncertainty axis more uniformly and facilitates frontier identification. Ultimately, the classification and ranking of locations is

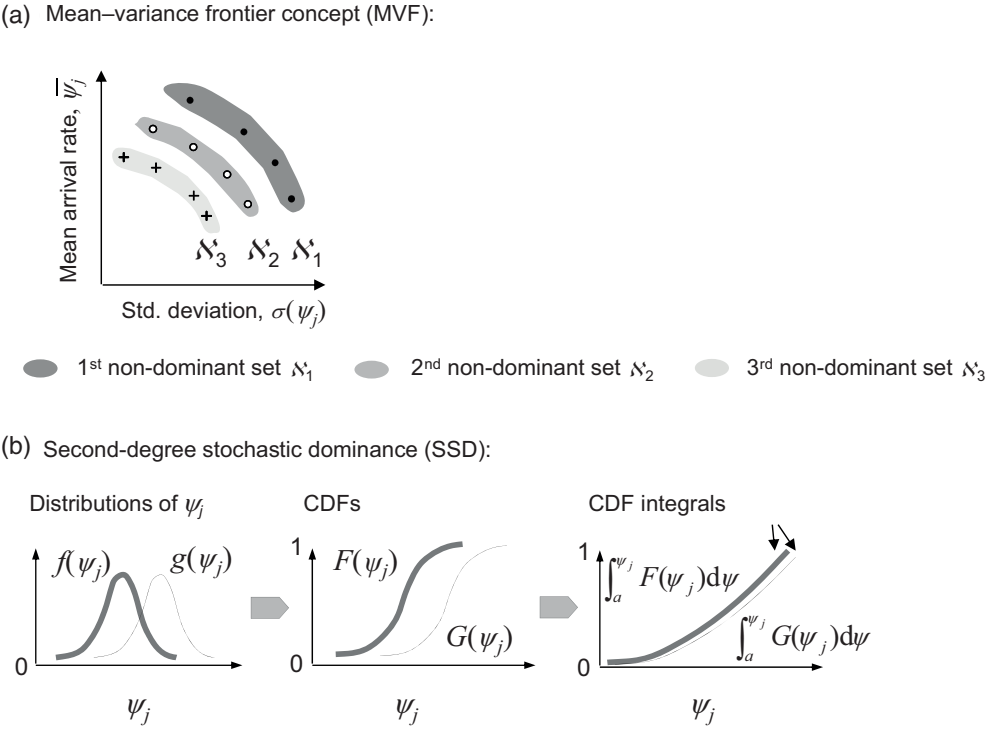

Fig. 14.2. The concepts of nested mean–variance frontiers and stochastic dominance: (a) ranking risk of invasion via nested frontiers in dimensions of mean risk and its standard deviation (i.e. risk-seeking preferences); (b) second-degree stochastic dominance rule. In (b), $f(\psi_j)$ and $g(\psi_j)$ are example distributions of pest arrival rates at two corresponding map locations, *f* and *g*; $F(\psi_j)$ and $G(\psi_j)$ are the cumulative distribution functions (CDFs) of $f(\psi_j)$ and $g(\psi_j)$; $\int_a^{\psi_j} F(\psi_j)\mathrm{d}\psi$ and $\int_a^{\psi_j} G(\psi_j)\mathrm{d}\psi$ are the integrals of the CDFs. The 'SSD' label highlights the second-order stochastic dominance condition (i.e. $\int_a^{\psi_j} F(\psi_j)\mathrm{d}\psi$ and $\int_a^{\psi_j} G(\psi_j)\mathrm{d}\psi$ do not cross each other).

similar whether the variance or standard deviation is used. The point, and corresponding map location, in the outer boundary of the cloud (i.e. the furthest from the origin) are assigned a priority rank of 1, the highest decision-making priority. Points that are an equivalent distance from the origin are also given a rank of 1. This set of priority 1 locations is removed from the mean–variance cloud, and the next set of points that are most distant from the origin in the new cloud are found and assigned rank 2, and so on. Each frontier represents a layer that has one-point width. The estimation of frontiers proceeds inwards one by one, like peeling an onion, as depicted in Fig. 14.2a, until all points are evaluated and assigned a corresponding priority rank. For the risk-seeking decision maker, the highest-priority locations are in the upper-outermost convex frontier of the mean–variance cloud (Fig. 14.2a). For risk-averse decision makers, the highest-priority locations are in the upper-innermost convex boundary where points exhibit extreme combinations of low variance and/or high mean values (Arrow, 1971; Elton and Gruber, 1995).

Stochastic dominance

Another popular technique to identify best-performing sets of portfolios is based on the second-degree stochastic dominance (SSD) rule. The SSD is a pair-wise ordering rule for distributions of observations. The SSD rule compares two distributions based on their cumulative distribution functions or CDFs (Fishburn and Vickson, 1978; Whitemore and Findlay, 1978; Levy, 1998). In our case, we compare two geographical locations, *f* and *g*. For each location, the assemblage of model-based invasion outcomes (i.e. across all of the model simulations) is described by the distribution, $f(\psi_j)$ or $g(\psi_j)$, of the pest arrival rate ψ_j, which can vary within an interval of values [*a*; *b*]. For simplicity, we consider a range of ψ_j values between 0 and 1, the absolute minimum and maximum values possible for this variable (Fig. 14.2b), but acknowledge that the range *a*–*b* can be broader if other metrics for pest risk are used. The SSD rule compares the distributions of *f* and *g* as represented by the integrals of their respective cumulative distribution functions:

$$\int_a^{\psi_j} F(\psi_j)\,\mathrm{d}\psi \quad \text{and} \quad \int_a^{\psi_j} G(\psi_j)\,\mathrm{d}\psi$$

where

$$F(\psi_j) = \int_a^{\psi_j} f(\psi_j)\,\mathrm{d}\psi \quad \text{and}$$

$$G(\psi_j) = \int_a^{\psi_j} g(\psi_j)\,\mathrm{d}\psi$$

Location *g* dominates the alternative *f* by second-degree stochastic dominance if

$$\int_a^{\psi_j} [F(\psi_j) - G(\psi_j)]\,\mathrm{d}\psi \geq 0 \text{ for all } \psi_j \quad \text{and}$$

$$\int_a^{\psi_j} [F(\psi_j) - G(\psi_j)]\,\mathrm{d}\psi > 0 \text{ for at least one } \psi_j \qquad (14.1)$$

Note that the integrals of the CDFs are calculated for the entire range of ψ_j values. For the SSD condition to be met, the integrals of the CDFs for $F(\psi_j)$ and $G(\psi_j)$ (i.e. lines depicting CDF integrals in Fig. 14.2b) must not cross. The SSD rule does not require $f(\psi_j)$ or $g(\psi_j)$ to be normally distributed. The rule also meets the assumptions of the risk-averse decision maker: given two choices with the same expected value, the more certain choice is always preferred (Levy, 1992; Levy and Levy, 2001). Because $G(\psi_j)$ and $F(\psi_j)$ represent the full distributions of model-based pest arrival rates at locations *f* and *g*, uncertainty in the ψ_j values may cause the dominance conditions to fail. Because *g* may not dominate *f* by the SSD rule it will end up with a comparatively lower rank due to the uncertainty (Levy, 1998).

For our example, potential differences in pest arrival rates ψ_j among locations were analysed by multiple, pair-wise SSD tests. For the test, one location was designated *f* and the other, *g*. By comparing all possible pairs of map locations (i.e. $n(n-1)$ pairs), we identified a subset ψ_1 that could not be dominated by any element in the rest of the set, $n - \aleph_1$, according to the SSD rule (i.e. that would make the dominance conditions

in Eqn 14.1 fail). After the first non-dominant subset ψ_1 was found, assigned a risk rank of 1 and removed from set n, the next non-dominant subset, $\aleph_2$, was found, assigned a risk rank of 2 and so on until all elements of n that represented the map locations were evaluated.

An Example with a Pathway-based Pest Invasion Model

We illustrate the portfolio-based methodology with a case study involving potential invasive alien species in Canadian forests. We use a relatively simple probabilistic model to estimate the likelihood that invasive forest insects may be carried in commercial freight transported to major Canadian municipalities via the North American road network. For simplicity, our model does not consider local pest spread by biological means or the pests' population dynamics. The choice of a particular model is not critical in demonstrating the portfolio-based approach. However, we have chosen a pathway-based model over more common spatial spread models because of its capacity for predicting human-assisted movement of invasive pests over long distances, a phenomenon that most spread models cannot predict well (Andow *et al*., 1990; Buchan and Padilla, 1999; Melbourne and Hastings, 2009). Pathway-based models describe the spread of a species through a network. The network is composed of nodes (e.g. a set of parks, campgrounds or cities) and connections between nodes. The network analysis prioritizes the degree of connectivity between the nodes (e.g. number of truck trips) over distance. So, for example, if 500 truck trips occur per day between cities A and C and only ten truck trips occur per day between A and B, a species is more likely to be moved from city A to city C than to city B even if city B is only 50 km from A and city C is 500 km from A. In general, pathway-based models can predict low-probability long-distance dispersal events better than common spatial spread models.

In our case, we associated the long-distance dispersal of invasive alien insect pests of forests with the movement of traded commodities via trucks on the North American road network. Traded commodities have been recognized as a reasonable predictor of the human-mediated movement of invasive species (e.g. Tatem *et al*., 2006; Hulme *et al*., 2008; Floerl *et al*., 2009; Hulme, 2009; Kaluza *et al*., 2010; Koch *et al*., 2011). We used a Commercial Vehicle Survey (CVS) maintained by Transport Canada as our primary data source to forecast movement of wood-boring forest pests with commodities and freight (Yemshanov *et al*., 2012a,b). We included commodity categories that involve raw wood products or are associated with significant quantities of wood packing materials (Table 14.1). These materials are acknowledged as a potential source of invasive alien forest pests, despite the implementation of International Standard for Phytosanitary Measures No. 15 (ISPM 15), which stipulates treatment of these materials to reduce the risk of pest introduction via international trade (USDA APHIS, 2000). The effectiveness of ISPM 15 has been questioned (Reaser and Waugh, 2007; Reaser *et al*., 2008), implying that such measures cannot completely eliminate risk (Haack and Petrice, 2009; Liebhold, 2012).

CVS data were collected during a 2005–2007 survey at truck weigh stations across Canada. Each CVS record summarized a single shipment route reported by a driver. The summary included the route origin, destination, (if applicable) the location(s) where the route crossed the US–Canadian border and a description of the cargo (i.e. type and tonnage). We selected records from the CVS database with commodity types that are commonly associated with invasive alien forest pests (Table 14.1). We reformatted the CVS data into a list of 'origin–destination' network segments so the location at the beginning of each segment (i.e. a part of a route from the CVS) was treated as an 'origin' and the location at the end of a segment as a 'destination' (Fig. 14.3). The network included about 11,000 individual locations in total.

We used the 'origin–destination' network to estimate the rate of transmission of

Table 14.1. Commodity categories from the US–Canadian Standard Classification of Transported Goods (SCTG) commonly associated with transport of bark- and wood-boring forest insects.

Commodity category (SCTG code)
Monumental or building stone (10)
Logs and other wood in the rough (25)
Wood products (26)
Non-metallic mineral products (31)
Base metal in primary or semi-finished forms and in finished basic shapes (32)
Articles of base metal (33)
Machinery (34)
Electronic and other electrical equipment and components and office equipment (35)
Motorized and other vehicles, including parts (36)
Transportation equipment, not elsewhere classified (37)
Precision instruments and apparatus (38)
Furniture, mattresses and mattress supports, lamps, lighting fittings (39)
Miscellaneous manufactured products (40)

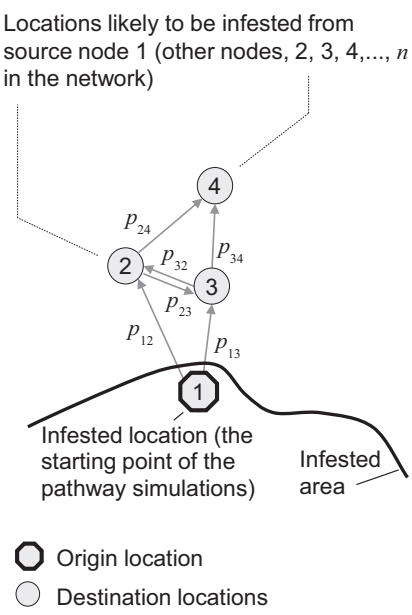

Fig. 14.3. Schematic representation of pest invasion spread in a network-based pathway model. The parameters p_{ij} represent the probability of movement from location *i* to location *j*.

invasive forest pests through an individual pathway segment between two given locations, *i* and *j*, in the network. We first summed the tonnages of forest pest-associated commodities recorded in the CVS data with one sum per directional pathway between locations *i* and *j*, which were designated m_{ij} and m_{ji} (note $m_{ij} \neq m_{ji}$). For each route segment *ij*, the rate, p_{ij}, of a forest pest being moved from *i* to *j* over the survey period (2005–2007) was estimated from the total tonnage of freight shipments of forest-pest-associated commodities from *i* to *j*:

$$p_{ij} = 1 - \exp(-m_{ij}\lambda_t) \tag{14.2}$$

where λ_t is the likelihood of a pest being moved with one tonne of relevant commodities over the survey period *t*. Essentially, λ_t is a multiplier that converts the tonnage value into a rate estimate. Given the scope of our case study (i.e. modelling the potential human-assisted movement of an entire class of forest pests) it is impossible to calculate an exact λ_t. However, because our primary focus was to prioritize locations

in terms of their relative potential to receive invasive forest pests from elsewhere (i.e. to establish a partial order among geographical locations in the transportation network), precise knowledge of λ_t was not critical (Yemshanov *et al*., 2012b). We used recent records of the spread of the emerald ash borer, a significant forest pest, along the most prominent vector of its expansion in Ontario, Canada (i.e. along the Highway 401 corridor between Windsor and Toronto), as well as the corresponding tonnages of relevant commodities moved through this corridor, to estimate λ_t (Yemshanov *et al*., 2012b). Briefly, we estimated λ_t via a series of iterative pathway model simulations that were intended to match the model-estimated and known rate of emerald ash borer spread along the Highway 401 corridor in southern Ontario given relevant trucking statistics.

Essentially, the model was comprised of a pathway matrix where each element p_{ij} estimates the rate of an invasive forest pest being moved with commercial truck transport from one geographical location, *i*, to another, *j*. The rows of the matrix represent the starting points of individual pathway segments, while the columns represent the segments' end points. The matrix also has an extra column that denotes the probability, p_{i0}, that the invasive organism fails to arrive at any location *j* from location *i*:

$$\mathbf{P}_t = \begin{bmatrix} 0 & p_{12} & \cdots & p_{1n} & p_{10} \\ p_{21} & 0 & \cdots & p_{2n} & p_{20} \\ \vdots & \vdots & \vdots & \vdots & \vdots \\ p_{n1} & p_{n2} & \cdots & 0 & p_{n0} \end{bmatrix} \quad (14.3)$$

where

$$p_{i0} = 1 - \sum_{j=1}^{n} p_{ij}$$

The introduction of the last column was required because the transmission probability values p_{ij} in a given row do not always sum to 1. Since the CVS data did not document the duration of stay at intermediate locations during transit, the diagonal elements of the matrix, p_{ii}, were not estimated. We left the p_{ii} values at zero and instead added a column with the p_{i0} values which bring the sum of each row to 1.

We used the pathway matrix to generate transmissions of a hypothetical invasive forest pest through the transportation network. The model generated discrete transmission pathways via multiple iterations. For each iteration, the model generated a single pathway route that started from an origin location *i* and passed through a number of destination locations until a location with no outgoing paths or the termination state based on the p_{i0} value was chosen. As depicted in Fig. 14.3, the model simulated the movement of the pest from each point of 'origin' *i* to other locations *j* by extracting the associated vector of probabilities p_{ij} (i.e. the row of matrix values associated with *i*) from the pathway matrix and using it to select the next pathway point. Finally, a rate of pest arrival was estimated from the number of times the pest arrived at *j* from *i* over multiple pathway simulations:

$$\varphi_{ij} = J_i / K \quad (14.4)$$

where J_i is the number of individual pathway simulations that started at location *i* and passed through location *j*. *K* is the total number of individual simulations of pathway spread from *i*. The value of *K* (i.e. 2×10^6 simulations for each origin point in this study) was limited by the available computing capacity.

The arrival rates were then rearranged so each *j* 'destination' in the transportation network was characterized by an empirical distribution, ψ_j, of pest arrival rates φ_{ij} from all other nodes *i*, $i \neq j$ (i.e. $n - 1$ locations). This distribution described the location's potential to receive a forest pest with commercial freight transported from elsewhere. Because each destination had a distribution of arrival rates simulated from one origin at a time, the level of uncertainty associated with each location *j* depends on the connectivity of the pathway network and the variation in commodity flows along the pathway segments. In order to generate a geographically continuous coverage, we aggregated point-based arrival rates into a 15 km × 15 km grid map by combining the ψ_j

values from each location into one common distribution. Each map cell was characterized by a distribution of ψ_j pest arrival rates from other map cells in Canada. We then applied our portfolio-based techniques, the mean–variance frontier and the stochastic dominance rule, to these distributions of arrival rates to rank geographical locations.

While we used portfolio-based techniques in our analyses for all of Canada, we only show the region in southern Ontario and Quebec with the highest traffic flows and road densities so that patterns can be illustrated more clearly (Fig. 14.4; see colour plate section). We express the risk ranks, $\iota_{j\ \mathrm{SSD}}$ and $\iota_{j\ \mathrm{MVF}}$, generated with the mean–variance and stochastic dominance rules, relative to the largest rank possible for each respective method. We have calculated the relative rankings, $r_{j\ \mathrm{MVF}}$ and $r_{j\ \mathrm{SSD}}$, as:

$$r_{j\ \mathrm{SSD}} = 1 - \{(\iota_{j\ \mathrm{SSD}} - 1) / \max[\iota_{j\ \mathrm{SSD}}]\};$$
$$r_{j\ \mathrm{MVF}} = 1 - \{(\iota_{j\ \mathrm{MVF}} - 1) / \max[\iota_{j\ \mathrm{MVF}}]\} \quad (14.5)$$

where $\max[\iota_{j\ \mathrm{SSD}}]$ and $\max[\iota_{j\ \mathrm{MVF}}]$ represent the maximum rank values in the SSD and MVF classifications. The relative rankings have values from 0 to 1, so the relatively highest-priority ranks are close to 1 and lowest are close to 0. These relative rankings are ordinal values and are meant to facilitate comparisons of MVF and SSD results.

To explore the geographic patterns of risk identified by the ranking methods we have further divided the ranks into broad classes with the arbitrary ranking thresholds of 0.4, 0.6, 0.75, 0.9 and 0.95 (Fig. 14.4; see colour plate section). Many of the highest ranked cells in eastern Canada ($r_{j\ \mathrm{MVF}}$, $r_{j\ \mathrm{SSD}} > 0.75$) are associated with major transportation arteries in southern Ontario and Quebec, which suggests that these corridors could serve as key pathways for new pest arrivals. The two ranking methods identified similar highest-priority areas (Fig. 14.4a and b); however, the map based on the SSD rule had more high-ranking sites (i.e. $r_{j\ \mathrm{SSD}} > 0.9$) than the map based on MVF. Table 14.2 illustrates the agreement between the priority rankings among the highest-ranked locations. (Note that each map cell was assigned a location name corresponding to the nearest large municipality.)

While the highest-ranked lists generated with the MVF and SSD rules are relatively close, they differed substantially from the ranks based only on the mean arrival rates.

We also compared maps of risk ranks derived with the MVF and SSD rules with the geographical distribution of the standard deviation of the arrival rates, $\sigma(\psi_j)$ (Fig. 14.4c; see colour plate section). Uncertainty, represented by standard deviation, figured prominently in location characterizations based on the MVF and SSD rules (Fig. 14.4a and b; see colour plate section); the highest-ranked locations typically included areas with high variability in pest arrival rates.

The impact of uncertainty on relative priority ranks, r_j, is even more evident when individual map locations are plotted as points on a graph of the mean pest arrival rate, $\bar{\psi}_j$, against the standard deviation, $\sigma(\psi_j)$ (Fig. 14.5). In Fig. 14.5a, the idealized boundaries between these general risk classes, as delineated with the MVF rule, are tilted at an angle, $\beta > 90°$, because the frontiers were selected starting with the upper-outermost boundary of the mean–variance cloud. This pattern shows that for any two locations with equal mean arrival rates, the location with higher variability would be assigned a higher priority rank, just as we had intended.

For delineations based on the SSD rule, the tilt angle β of the boundaries between the risk classes was below 90° (Fig. 14.5b). This result implies that for any two locations with equal mean arrival rates, the location with the more certain estimate (i.e. with lower variability) would be assigned a higher rank.

In summary, the two approaches perform similarly in terms of the highest- and lowest-ranked locations, but for moderate risk ranks, the methods place differing levels of emphasis on certainty in the arrival rate estimate (i.e. the MVF approach emphasizes areas of high

Table 14.2. Location rankings for Canadian cities based on mean arrival rate, mean–variance frontiers (MVF) and second-degree stochastic dominance (SSD) methods. A ranking based only on the locations' mean arrival rate values is included for comparison.

	Ranking method							Ranking method					
	Mean arrival rate		MVF		SSD			Mean arrival rate		MVF		SSD	
Location name[a]	ψ_j ($\times 10^{-5}$)	r_j^b	Rank	r_j	Rank	r_j	Location name (continued)	ψ_j ($\times 10^{-5}$)	r_j	Rank	r_j	Rank	r_j
Cornwall, ON	15.9	145*	1	1	16*	1	Gananoque, ON	35.0	2	20	0.91	32	0.94
Toronto, ON	65.3	1	2	0.995	1	1	Ottawa, ON	7.7	38	32	0.88	18	0.96
Windsor, ON	29.8	3	4	0.98	1	1	Calgary, AB	21.4	8	14	0.94	56	0.9
Kitchener, ON	21.2	9	3	0.99	6	0.99	Oshawa, ON	23.9	5	26	0.89	31	0.94
Drummondville, QC	7.6	39	5	0.98	11	0.98	Nobleton, ON	2.3	80	45	0.86	15	0.96
Trois-Rivieres, QC	8.9	30	7	0.97	7	0.99	Sorel, QC	2.0	89	41	0.86	20	0.96
Iroquois, ON	6.0	45	8	0.96	5	0.99	White Rock, BC	22.6	7	21	0.91	60	0.89
Moncton, NB	9.1	28	6	0.97	10	0.98	Niagara Falls, ON	5.5	13	33	0.87	34	0.93
Ste Madeleine, QC	11.1	22	10	0.95	8	0.99	Abbotsford, BC	19.9	11	23	0.91	68	0.88
Quebec, QC	8.3	34	15	0.93	1	1	Kingston, ON	13.8	18	31	0.88	47	0.91
Montreal, QC	15.8	15	9	0.95	9	0.98	Sault Ste Marie, ON	12.5	20	40	0.86	42	0.92
Sarnia, ON	23.4	6	13	0.94	14	0.97	Orono, ON	14.0	17	50	0.85	44	0.92
Lacolle, QC	4.8	52	11	0.94	12	0.97	Sparwood, BC	10.4	24	25	0.9	76	0.86
London, ON	26.8	4	12	0.94	19	0.96	Ingersoll, ON	19.8	12	36	0.87	63	0.89
Hamilton, ON	14.8	16	18	0.92	13	0.97	Thunder Bay, ON	9.1	27	44	0.86	140	0.79
St Georges, QC	2.6	73	16	0.93	16	0.96	Halifax, NS	1.6	102	42	0.86	36	0.93
Napanee, ON	21.0	10	17	0.92	23	0.95	Winnipeg, MB	8.4	32	30	0.88	49	0.91
Windsor, QC	7.3	42	22	0.91	17	0.96	Edmonton, AB	8.2	35	54	0.84	87	0.85
North Bay, ON	13.5	19	19	0.92	24	0.95	Vancouver, BC	6.4	43	57	0.83	96	0.84

The list is sorted by the sum of $r_{j\,\mathrm{MVF}}$ and $r_{j\,\mathrm{SSD}}$ values.

[a]Location name based on nearest large municipality at 15 km spatial resolution: AB, Alberta; BC, British Columbia; MB, Manitoba; NB, New Brunswick; NS, Nova Scotia; ON, Ontario; QC, Quebec.

[b]r_j, relative rank denotes the location's rank order relative to the total number of ranks for that metric. Values nearest 1.0 are the highest priority.

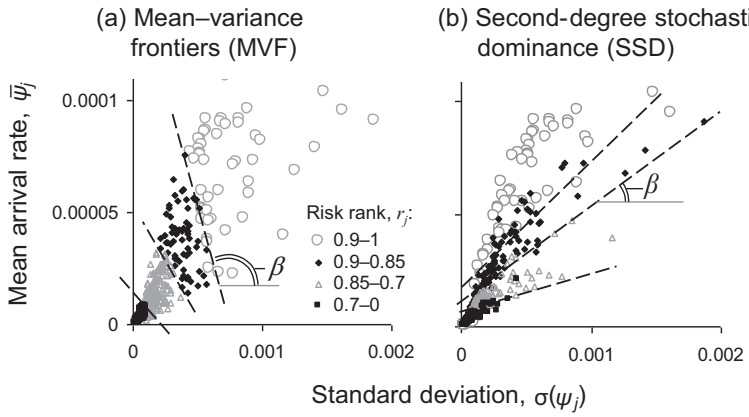

Fig. 14.5. Relative pest risk ranks, r_j, for each location, *j*, plotted with respect to mean pest arrival rate, $\bar{\psi}_j$, and its standard deviation, $\sigma(\psi_j)$. β denotes the tilt angle between the idealized boundaries of coarsely defined risk classes in the mean–variance cloud and the line indicating constant mean arrival rate ($\bar{\psi}_j$ = const). Different symbols delineate broad classes of the risk ranks and dashed lines depict idealized boundaries between broad classes of risk ranks.

uncertainty more). This distinctive behaviour occurs because the delineation of the non-dominant sets in the MVF and SSD classifications effectively starts from the opposite sides of the mean–variance cloud and thus the two methods offer different treatments of uncertainty.

Assessing the Utility of Portfolio-based Techniques for Pest Risk Assessment

Historically, the adoption of portfolio-based techniques in economic studies was driven by the need to find the best possible allocation of financial assets in the context of uncertain returns (Levy and Markowitz, 1979; Götze *et al.*, 2008). The idea of incorporating decision-making priorities as a component of financial predictive models applies well to other decisions that have to be made under uncertainty. In our model-based assessment of the likelihood of pest arrival, portfolio-based approaches provided a tractable way to incorporate uncertainty into quantitative assessments of the relative risk of pest arrival among several sites that is consistent with decision-making priorities and to communicate those differences in a single decision support product (i.e. a map of relative priority ranks in our study).

In economics, if the objective is to find the smallest set of best-performing investment portfolios, the SSD and MVF approaches have been criticized as too coarse to be practical (Hardaker *et al.*, 2004; Hardaker and Lien, 2010). However, we found the discriminatory power of SSD and MVF rules to be sufficient for our pest risk modelling case. Since our study required ranking of all geographic locations in the map and the total number of locations was large, SSD and MVF rules were sufficient to identify geographical hot spots as small as a few adjacent map cells. Also, the magnitude of the variation in the pest arrival rate values was considerably larger than the typical volatility associated with investment analyses; hence differences between the CDF integrals in the case of the SSD rule and convex mean–variance frontiers in the case of the MVF approach were more discernible.

In our example, we demonstrated how the incorporation of uncertainty via the MVF and SSD methods can change the interpretation of geographical estimates of the pest arrival risk. The output pest arrival risk was a dimensionless priority rank aimed to assist decision makers with allocations of

resources for pest surveillance and control. Maps of risk ranks can be used as inputs for further economic assessments of survey costs which may include optimization of resources for survey and pest control efforts. The methodology might be used with a cost-based metric that estimates potential benefits of successful detections or management actions in response to an outbreak, culminating in an optimal cost allocation study.

The capacity of the portfolio-based techniques to account for uncertainty also improves the utility of stochastic invasion models (Demeritt *et al*., 2007) as risk assessment and decision support tools. We illustrated the methods with a relatively simple invasion model, but the approach can be linked to more complex, probabilistic models where uncertainty in model predictions is expected to be high. Similarly, the approach could be used with spatial models to generate plausible invasion outcomes at multiple geographical locations. For example, stochastic cellular automata and gravity models (e.g. Haynes and Fotheringham, 1984; Muirhead *et al*., 2006; Pitt *et al*., 2009; Yemshanov *et al*., 2009a) could generate multiple maps, each representing a possible outcome of the invasion process. Multiple maps can be rearranged so each geographical location is characterized by a distribution of invasion likelihoods or impact metrics which could be used with one of the portfolio-based techniques presented here.

Incorporating decision makers' perceptions of uncertainty

The MVF and the SSD techniques can address decision-making strategies where uncertainty is treated differently. The MVF approach, as implemented in this study, may be suitable when the uncertainty about a pest is a factor that might increase the priority for decision makers. In particular, the MVF concept is useful when both the central tendency (i.e. the mean) and variability (e.g. the standard deviation) of the risk metric represent critical decision-making variables. For instance, the MVF approach could be applied in model-based assessments for early detection of invasive organisms, when the need to gain more information and reduce uncertainty about the invader's presence or absence is paramount. In such cases, the model-based rate of pest arrival may not sufficiently characterize information gains from unexpected events such as detections of a pest in low-probability locations. Consequently, the uncertainty of the arrival rate estimate becomes a distinctly important variable, so the prioritization should include arrival rate and its variance. Alternatively, delineation based on the SSD rule may be more suitable for assessments that support costly and irreversible decisions such as restricting trade or imposing a regulation, or when decision makers are risk-averse.

Ultimately, the applicability of a particular portfolio-based method can be affected by the type of pest invasion model and the nature of the model output used in the assessment. One analytical strategy that may be worth considering is to estimate the priority ranks with more than one algorithm and then undertake an extra analysis step of aggregating the multiple sets of output ranks into a single-dimensional decision priority metric using multi-criteria aggregation techniques that do not require prior setting of the criteria weights (e.g. the multi-attribute frontier aggregation described in Yemshanov *et al*., 2013).

Computational remarks

Both the MVF and SSD techniques perform a delineation of nested efficient frontiers for a particular map (i.e. a particular set of spatial elements), which means they only rank those elements relative to one another. In order to compare the maps of multiple scenarios or different geographical regions, the priority ranks would need to be remapped to a new common scale. The simplest approach would be to combine all geographical sets or scenarios into a single superset that includes all alternative maps or scenario data sets, and then assign the

priority ranks with respect to all possible invasion outcomes and scenarios that could be found in this superset.

The MVF and SSD techniques use somewhat different approaches to generate the rank values. The MVF approach essentially 'peels' the mean–variance cloud of points, starting from the outermost layer. Alternatively, the stochastic dominance approach ranks the geographical locations via multiple pair-wise SSD tests. As a consequence, the two techniques typically yield different numbers of locations at the highest ranks. For example, Table 14.2 lists eight locations with priority ranks above 0.95 for the MVF-based classification versus 20 locations for the SSD-based approach. The allocation of the frontiers in the MVF approach can also be influenced by local variations of the point density in the mean–variance space: more frontiers can be delineated in regions of the mean–variance space with higher point density. Also note that the MVF rule assumes that the mean values and the variance provide an adequate representation of the distribution as a whole (Gandhi and Saunders, 1981). Alternatively, the stochastic dominance approach evaluates the entire cumulative distribution of expected outcomes and does not require prior evaluation of the distribution shape (Fishburn and Vickson, 1978).

The application of either the SSD or MVF approach to large geographical data sets, such as high-resolution outputs of invasion and dispersal models with a large number of spatial elements (i.e. map cells or polygons), is computationally demanding[1]. For example, the SSD test has a computational complexity on the order of $n(n-1)/2$ and the most basic algorithm to find two-dimensional convex MVF frontiers has a complexity on the order of n^2. For very large data sets, further reduction of the computing time is possible by implementing more efficient convex frontier delineation algorithms (Porter *et al.*, 1973; Kung *et al.*, 1975; Rhee *et al.*, 1995; Papadias *et al.*, 2003).

Acknowledgements

The authors extend their gratitude and thanks to Kirsty Wilson and Marty Siltanen (Natural Resources Canada, Canadian Forest Service) for technical support and diligence with preparing the CVS data set for this case study. The participation of Denys Yemshanov was supported by an interdepartmental NRCan–CFIA Forest Invasive Alien Species initiative. The participation of Mark Ducey was supported by the Agriculture and Food Research Initiative Competitive Grants Program Grant No. 2010-85605-20584 from the National Institute of Food and Agriculture.

Notes

[1] Software that performs basic MVF and SSD rankings can be obtained from the lead author at Denys.Yemshanov@NRCan-RNCan.gc.ca.

References

Andow, D.A., Kareiva, P.M., Levin, S.A. and Okubo, A. (1990) Spread of invading organisms. *Landscape Ecology* 4, 177–188.

Arrow, K.J. (1971) *Essays in the Theory of Risk Bearing*. Markham, Chicago, Illinois.

Buchan, L.A.J. and Padilla, D.K. (1999) Estimating the probability of long-distance overland dispersal of invading aquatic species. *Ecological Applications* 9, 254–265.

Demeritt, D., Cloke, H., Pappenberger, F., Theilen, J., Bartholmes, J. and Ramos, M.-H. (2007) Ensemble predictions and perceptions of risks, uncertainty, and error in flood forecasting. *Environmental Hazards* 7, 115–127.

Elton, E.J. and Gruber, M.J. (1995) *Modern Portfolio Theory and Investment Analysis*, 5th edn. Wiley, New York.

Fishburn, P.C. and Vickson, R.C. (1978) Theoretical foundations of stochastic dominance. In: Whitemore, G.A. and Findlay, M.C. (eds) *Stochastic Dominance: An Approach to Decision-Making under Risk*. Lexington Books, D.C. Heath and Co., Lexington, Massachusetts, pp. 39–144.

Floerl, O., Inglis, G.J., Deym K. and Smith, A. (2009) The importance of transport hubs in stepping-stone invasions. *Journal of Applied Ecology* 46, 37–45.

Gandhi, D.K. and Saunders, A. (1981) The superiority of stochastic dominance over mean variance efficiency criteria: some clarifications. *Journal of Business Finance & Accounting* 8, 51–59.

Gigerenzer, G. (2002) *Calculated Risks: How to Know When Numbers Deceive You*. Simon & Schuster, New York.

Goldberg, D.E. (1989) *Genetic Algorithms in Search, Optimization, and Machine Learning*. Addison-Wesley, Reading, Massachusetts.

Götze, U., Northcott, D. and Schuster, P. (2008) *Investment Appraisal – Methods and Models*. Springer, Berlin.

Haack, R.A. and Petrice, T.R. (2009) Bark- and wood-borer colonization of logs and lumber after heat treatment to ISPM 15 specifications: the role of residual bark. *Journal of Economic Entomology* 102, 1075–1084.

Hardaker, J.B. and Lien, G. (2010) Stochastic efficiency analysis with risk aversion bounds: a comment. *Australian Journal of Agricultural and Resource Economics* 54, 379–383.

Hardaker, J.B., Richardson, J.W., Lien, G. and Schumann, K.D. (2004) Stochastic efficiency analysis with risk aversion bounds: a simplified approach. *Australian Journal of Agricultural and Resource Economics* 48, 253–270.

Haynes, K.E. and Fotheringham, A.S. (1984) *Gravity and Spatial Interaction Models*. Sage, Beverly Hills, California.

Hulme, P.E. (2009) Trade, transport and trouble: managing invasive species pathways in an era of globalization. *Journal of Applied Ecology* 46, 10–18.

Hulme, P.E., Bacher, S., Kenis, M., Klotz, S., Kuhn, I., Minchin, D., Nentwig, W., Olenin, S., Panov, V., Pergl, J., Pysek, P., Roques, A., Sol, D., Solarz, W. and Vila, M. (2008) Grasping at the routes of biological invasions: a framework for integrating pathways into policy. *Journal of Applied Ecology* 45, 403–414.

Ingersoll, J.E. Jr (1987) *Theory of Financial Decision Making*. Rowman & Littlefield, Lanham, Maryland.

Kahneman, D. and Tversky, A. (1979) Prospect theory of decisions under risk. *Econometrica* 47, 263–291.

Kahneman, D., Slovic, P. and Tversky, A. (1982) *Judgment Under Uncertainty: Heuristics and Biases*. Cambridge University Press, New York.

Kaluza, P., Kolzsch, A., Gastner, M.T. and Blasius, B. (2010) The complex network of global cargo ship movements. *Journal of the Royal Society Interface* 7, 1093–1103.

Koch, F.H., Yemshanov, D., McKenney, D.W. and Smith, W.D. (2009) Evaluating critical uncertainty thresholds in a spatial model of forest pest invasion risk. *Risk Analysis* 29, 1227–1241.

Koch, F.H., Yemshanov, D., Colunga-Garcia, M., Magarey, R.D. and Smith, W.D. (2011) Establishment of alien-invasive forest insect species in the United States: where and how many? *Biological Invasions* 13, 969–985.

Kung, H.T., Luccio, F. and Preparata, F.P. (1975) On finding the maxima of a set of vectors. *Journal of the Association for Computing Machinery* 22, 469–476.

Levy, H. (1992) Stochastic dominance and expected utility: survey and analysis. *Management Science* 38, 555–593.

Levy, H. (1998) *Stochastic Dominance: Investment Decision Making under Uncertainty*. Kluwer Academic Publishers, Dordrecht, The Netherlands.

Levy, H. and Markowitz, H. (1979) Approximating expected utility by a function of mean and variance. *The American Economic Review* 69, 308–317.

Levy, M. and Levy, H. (2001) Testing for risk aversion: a stochastic dominance approach. *Economics Letters* 71, 233–240.

Liebhold, A.M. (2012) Forest pest management in a changing world. *International Journal of Pest Management* 58, 289–295.

Melbourne, B.A. and Hastings, A. (2009) Highly variable spread rates in replicated biological invasions: fundamental limits to predictability. *Science* 325, 1536–1539.

Muirhead, J.R., Leung, B., van Overdijk, C., Kelly, D.W., Nandakumar, K., Marchant, K.R. and MacIsaac, H.J. (2006) Modelling local and long-distance dispersal of invasive emerald ash borer *Agrilus planipennis* (Coleoptera) in North America. *Diversity and Distributions* 12, 71–79.

Papadias, D., Tao, Y., Fu, G. and Seeger, B. (2003) An optimal and progressive algorithm for skyline queries. *Proceedings of the 2003 Association for Computing Machinery Special Interest Group on Management*. International Conference on Management of Data, San Diego, California, pp. 467–478.

Pitt, J.P.W., Worner, S.P. and Suarez, A.V. (2009) Predicting Argentine ant spread over the heterogeneous landscape using a spatially explicit stochastic model. *Ecological Applications* 19, 1176–1186.

Porter, R.B., Wart, J.R. and Ferguson, D.L. (1973) Efficient algorithms for conducting stochastic

dominance tests on large numbers of portfolios. *Journal of Financial and Quantitative Analysis* 8, 71–81.

Prasad, A.M., Iverson, L.R., Peters, M.P., Bossenbroek, J.M., Matthews, S.N., Syndor, T.D. and Schwartz, M.W. (2010) Modeling the invasive emerald ash borer risk of spread using a spatially explicit cellular model. *Landscape Ecology* 25, 353–369.

Rafoss, T. (2003) Spatial stochastic simulation offers potential as a quantitative method for pest risk analysis. *Risk Analysis* 23, 651–661.

Reaser, J.K. and Waugh, J. (2007) *Denying Entry: Opportunities to Build Capacity to Prevent the Introduction of Invasive Species and Improve Biosecurity at US Ports*. International Union for Conservation of Nature (IUCN), Gland, Switzerland.

Reaser, J.K., Meyerson, L.A. and Von Holle, B. (2008) Saving camels from straws: how propagule pressure-based prevention policies can reduce the risk of biological invasion. *Biological Invasions* 11, 193–203.

Rhee, C., Dhall, S.K. and Lakshmivarahan, S. (1995) The minimum weight dominating set problem for permutation graphs is in *NC*. *Journal of Parallel and Distributed Computing* 28, 109–112.

Shefrin, H. and Belotti, M.L. (2007) Behavioral finance: biases, mean–variance returns, and risk premiums. *CFA Institute Publications* 2007 (June), 4–12.

Tatem, A.J., Rogers, D.J. and Hay, S.I. (2006) Global transport networks and infectious disease spread. *Advances in Parasitology* 62, 293–343.

USDA APHIS (2000) *Pest Risk Assessment for Importation of Solid Wood Packing Materials into the United States*. US Department of Agriculture, Animal Plant Health Inspection Service, Plant Protection Quarantine, Riverdale, Maryland.

Venette, R.C., Kriticos, D.J., Magarey, R., Koch, F.H., Baker, R.H.A., Worner, S.P., Gómez, N.N., McKenney, D.W., Dobesberger, E.J., Yemshanov, D., De Barro, P.J., Hutchison, W.D., Fowler, G., Kalaris, T.M. and Pedlar, J. (2010) Pest risk maps for invasive alien species: a roadmap for improvement. *BioScience* 60, 349–362.

Whitemore, G.A. and Findlay, M.C. (1978) Introduction. In: Whitemore, G.A. and Findlay, M.C. (eds) *Stochastic Dominance: An Approach to Decision-Making under Risk*. Lexington Books, D.C. Heath and Co., Lexington, Massachusetts, pp. 1–36.

Yemshanov, D., Koch, F.H., McKenney, D.W., Downing, M.C. and Sapio, F. (2009a) Mapping invasive species risks with stochastic models: a cross-border United States–Canada application for *Sirex noctilio* Fabricius. *Risk Analysis* 29, 868–884.

Yemshanov, D., McKenney, D.W., De Groot, P., Haugen, D.A., Sidders, D. and Joss, B. (2009b) A bioeconomic approach to assess the impact of an alien invasive insect on timber supply and harvests: a case study with *Sirex noctilio* in eastern Canada. *Canadian Journal of Forest Research* 39, 154–168.

Yemshanov, D., Koch, F.H., Ben-Haim, Y. and Smith, W.D. (2010) Detection capacity, information gaps and the design of surveillance programs for invasive forest pests. *Journal of Environmental Management* 91, 2535–2546.

Yemshanov, D., Koch, F.H., Lyons, B., Ducey, M. and Koehler, K. (2012a) A dominance-based approach to map risks of ecological invasions in the presence of severe uncertainty. *Diversity and Distributions* 18, 33–46.

Yemshanov, D., Koch, F.H., Ducey, M. and Koehler, K. (2012b) Trade-associated pathways of alien forest insect entries in Canada. *Biological Invasions* 14, 797–812.

Yemshanov, D., Koch, F.H., Ben-Haim, Y., Downing, M. and Sapio, F. (2013) A new multicriteria risk mapping approach based on a multiattribute frontier concept. *Risk Analysis* 33, 1694–1709.